

Heavy QCD Axion at Belle II: Displaced and Prompt Signals

Emilie Bertholet,¹ Sabyasachi Chakraborty,^{2,3} Vazha Lomadze,²
Takemichi Okui,^{2,4} Abner Soffer,¹ and Kohsaku Tobioka^{2,4}

¹*Tel Aviv University, School of Physics and Astronomy, Tel Aviv, 69978, Israel*

²*Department of Physics, Florida State University, Tallahassee, FL 32306, USA*

³*SISSA International School for Advanced Studies, Via Bonomea 265, 34136, Trieste, Italy*

⁴*Theory Center, High Energy Accelerator Research Organization (KEK), Tsukuba 305-0801, Japan*

The QCD axion is a well-motivated addition to the standard model to solve the strong CP problem. If the axion acquires mass dominantly from a hidden sector, it can be as heavy as $O(1)$ GeV, and the decay constant can be as low as $O(100)$ GeV without running into the axion quality problem. We propose new search strategies for such heavy QCD axions at the Belle II experiment, where the axions are expected to be produced via $B \rightarrow Ka$. We find that a subsequent decay $a \rightarrow 3\pi$ with a displaced vertex leads to a unique signal with essentially no background, and that a dedicated search can explore the range $O(1-10)$ TeV of decay-constant values. We also show that $a \rightarrow \gamma\gamma$ can cover a significant portion of currently unexplored region of $150 \lesssim m_a \lesssim 500$ MeV.

I. INTRODUCTION

The axion is one of the most well-motivated hypothetical particles beyond the standard model (SM) of particle physics. The original axion was predicted by Weinberg and Wilczek [1, 2] as the pseudo-Nambu-Goldstone boson of the spontaneously broken $U(1)$ symmetry proposed by Peccei and Quinn [3, 4] to solve the strong CP problem [5]. While the axion could have additional couplings to the SM particles, the minimal effective Lagrangian thus motivated, up to terms to be included for renormalization, is given by

$$\mathcal{L} = \mathcal{L}_{\text{SM}} + \frac{\alpha_s}{8\pi} \frac{a}{f_a} G\tilde{G} + \frac{1}{2}(\partial_\mu a)^2 - \frac{m_a^2}{2}a^2, \quad (1)$$

where a is the axion, with mass m_a and decay constant f_a , and G is the gluon. Such an axion, which we call the *QCD axion*, is the subject of this paper.

Most phenomenological studies and experimental searches for the QCD axion have so far focused on *light* axion masses [6, 7], i.e., $m_a < 3m_\pi$, where the physics is dominated by the axion-photon-photon coupling necessarily induced upon QCD confinement, even though the underlying Lagrangian (1) lacks such coupling. This coupling provides various experimental handles, such as the $a \rightarrow \gamma\gamma$ decay and the axion-photon conversion in a background magnetic field.

There are, however, good reasons to explore *heavy* axion masses, $m_a > 3m_\pi$, where hadronic physics controls the phenomenology. In particular, such a heavy QCD axion can provide a simple solution [8] to the *axion quality problem* [9–12], i.e., the violation of the $U(1)$ Peccei-Quinn symmetry by higher dimensional Planck-suppressed operators induced (presumably) by quantum gravity. Such violation should become harmless if $f_a \lesssim O(10)$ TeV [8], but this would imply $m_a \gtrsim O(1)$ keV due to the relation $m_a \sim m_\pi f_\pi / f_a$, if the axion mass is induced solely by QCD. This part of the parameter space, however, is excluded by beam dump experiments [13–15] and astrophysical observations [16–19]. The simplest way

out is to introduce additional contributions to the axion mass, such that $m_a \gg m_\pi f_\pi / f_a$ [8]. For our purpose, this simply amounts to treating m_a and f_a in the Lagrangian (1) as independent parameters. Such treatment can be justified by (small modifications of) many ultraviolet (UV)-complete models, such as those in Refs. [8, 20–23]. Also, a heavy QCD axion could be relevant to inflation, and in this case the interesting parameter is $m_a \sim 10^{-6} f_a$ [24].

In searching for a heavy QCD axion experimentally, the presence of the $aG\tilde{G}$ coupling in Eq. (1) implies that the predominant axion production should be hadronic. As a result, experiments such as proton beam dump [15, 25], kaon decays [26–34], precision measurements of pion decays [35–37], fixed target [25, 38, 39], and colliders [25, 40, 41] set strong bounds on f_a . For $m_a \gtrsim 50$ GeV the CMS dijet search excludes large regions of parameter space [42, 43].

On the other hand, the range $O(100)$ MeV $\lesssim m_a \lesssim 50$ GeV is poorly constrained. For $m_a > 400$ MeV the kaon and beam-dump experiments are not very effective, and in fact, the strongest probe to-date is from $B \rightarrow Ka$. The study of this channel was pioneered in Ref. [25], where the underlying $b \rightarrow sa$ amplitude was estimated and the branching fractions of the subsequent a decay into various final states were inferred by a data-driven method. The leading-order determination of the $b \rightarrow sa$ amplitude requires a 2-loop calculation and leading 2-loop renormalization group evolution with varying initial conditions for the evolution. This was performed in Ref. [44], where the result was combined with the data-driven branching fractions of [25] to derive constraints from the past B -factory results and future projections for Belle II for the prompt axion decays $a \rightarrow \pi^0\pi^+\pi^-$, $\eta\pi^+\pi^-$, $KK\pi$, and $\phi\phi$. Finally, axion production in $\phi \rightarrow \gamma a$ and $\eta' \rightarrow \pi\pi a$ also sets constraints on the parameter space [45].

In this paper, we aim to significantly extend the study of prospects of future searches at Belle II, which was discussed in Ref. [44]. In particular, we show that displaced

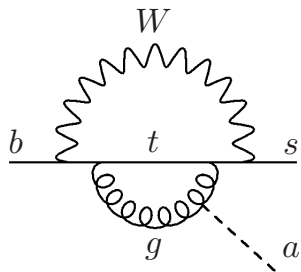


FIG. 1. A representative diagram of the leading contribution to the $b \rightarrow sa$ process from the Lagrangian (1).

axion decays to $\pi^0\pi^+\pi^-$ should provide a powerful search strategy, since the axion tends to be long-lived in the parameter space of our interest, and hence this signature is associated with little background. The prompt and displaced axion decays $a \rightarrow \gamma\gamma$ is another promising signature to probe an allowed region at $m_a < 3m_\pi$. Since this channel was not explored in the previous work [44], we study its potential here.

II. SUMMARY OF $B \rightarrow K^{(*)}a$ THEORY CALCULATION

Here we summarize the theoretical results of Ref. [44]. From the Lagrangian (1), the leading contribution to the process $b \rightarrow sa$ arises at 2-loop order, a representative diagram being shown in Fig. 1. The $b \rightarrow sa$ amplitude is captured by the following effective operator at scales below M_W :

$$\mathcal{L}_{bsa} = C \frac{\partial_\mu a}{f_a} \bar{s}_L \gamma^\mu \gamma_5 b_L + \text{h.c.} \quad (2)$$

with

$$C = C_{bs}(\mu) + \frac{\alpha_w}{4\pi} C_{qq}(\mu) g(\mu) + \frac{1}{2} \frac{\alpha_w}{4\pi} \left(\frac{\alpha_s}{4\pi} \right)^2 f(\mu). \quad (3)$$

Here, $\mu \sim M_W$, and we refer the reader to Appendix B of Ref. [44] for the (lengthy) expressions of the functions $f(\mu)$ and $g(\mu)$. The coefficients $C_{qq}(\mu)$ and $C_{bs}(\mu)$ are required by renormalization of the 2-loop diagrams, the former being the coefficient of the $(\partial_\mu a/f_a) \bar{q} \gamma^\mu \gamma_5 q$ counterterm, and the latter being that of $(\partial_\mu a/f_a) \bar{s}_L \gamma^\mu \gamma_5 b_L$. Physically, these two coefficients parametrize the inevitably model-dependent effects of the UV physics that supersedes the low energy description, Eq. (1), above some high scale Λ_{UV} . Rather than committing to a particular UV model, Ref. [44] varies the “initial conditions”, $C_{qq}(\Lambda_{UV})$ and $C_{bs}(\Lambda_{UV})$, over their natural ranges and uses the renormalization group evolution of $C_{qq}(\mu)$ and $C_{bs}(\mu)$ to study the impact of the unknown UV physics on the bounds on m_a and f_a extracted in the infrared. To go from the $b \rightarrow sa$ amplitude to the $B \rightarrow K^{(*)}a$ branching fraction, the result above is then combined with form

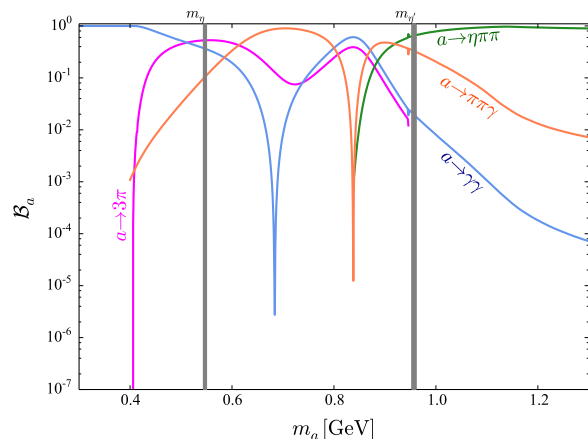


FIG. 2. Heavy QCD axion branching fractions as a function of its mass, taken from [25]. The decay modes relevant to our analyses are $a \rightarrow 3\pi$, $\gamma\gamma$, and $\eta\pi\pi$.

factors obtained from the light-cone QCD sum rules [46–49]. An approximate formula for the branching fraction based on Eq. (8) of Ref. [44] with $A = +3$ and $B = -3$ is given by

$$\text{BR}(B^+ \rightarrow K^+ a) \simeq 2(10) \times 10^{-5} \left(\frac{100 \text{ GeV}}{f_a} \right)^2, \quad (4)$$

for $\Lambda_{UV} = 1(10)$ TeV, respectively.

III. AXION DECAYS: DISPLACED AND PROMPT

Due to its coupling to gluons, the decays of a heavy QCD axion are very diverse [25]. In terms of the ranges of m_a , we can summarize the decay patterns as follows.

For $3m_\pi < m_a < m_\eta + 2m_\pi \sim 900$ MeV, the branching fraction of $a \rightarrow 3\pi$ is sizable, as shown in Fig. 2. In this mass range, with f_a in the range of our interest $1 \lesssim f_a \lesssim 10$ TeV, the axion can give rise to a displaced vertex signature in the Belle II detector. Because of the displacement, one can optimize experimental cuts to reduce the background considerably. Consequently, analyzing displaced $B \rightarrow Ka(3\pi)$ can result in very strong bounds on f_a . For higher f_a the axion would be effectively invisible, a signature for which detection methods exist, but with very low efficiency [50]. Furthermore, as seen from Eq. (4), the production rate of the axion in this case is too small even with the full data set of Belle II. Hence, the channel $B \rightarrow Ka(\text{invisible})$ is unfavorable, unless other couplings than in Eq. (1) increase the axion production.

For $m_a > m_\eta + 2m_\pi$, the decay mode of $a \rightarrow \eta\pi\pi$ quickly dominates, and the axion lifetime becomes shorter. This channel was studied in Ref. [44].

For $m_a < 3m_\pi$, $a \rightarrow 2\gamma$ dominates.¹ Thus, to search for a heavy QCD axion with mass below ~ 400 MeV one has to study the diphoton final state.

Following Ref. [25], we exclude few-MeV-wide regions of m_a around m_η and $m_{\eta'}$, because a large mixing of a with η or η' would invalidate the perturbative treatment.

To summarize, in this paper, we present projections for the reach of Belle II using displaced $B \rightarrow Ka(3\pi)$ decays, and $B \rightarrow Ka(\gamma\gamma)$ decays that may be prompt or displaced.

A. Displaced $B^- \rightarrow K^- a(\pi^+ \pi^- \pi^0)$ signature

In the mass range $3m_\pi < m_a < m_\eta + 2m_\pi$, we propose to search for the long-lived axion in $B^- \rightarrow K^- a$ with $a \rightarrow \pi^+ \pi^- \pi^0$. The two charged pions form a displaced vertex (DV) significantly away from the interaction point of the e^+e^- beams. The DV is also the production point of the two photons that originate from the π^0 decay. Following the usual practice of B -meson reconstruction at e^+e^- B -factories, signal identification will rely on the variables $\Delta E \equiv E_B - \sqrt{s}/2$ and $M_{bc} \equiv \sqrt{s/4 - p_B^2}$, where s is the center-of-mass energy of the e^+e^- collision, and E_B and p_B are the measured energy and momentum of the B candidate in the center-of-mass frame.

1. Background

To estimate the background for this search, we start from the Belle Collaboration study of $B \rightarrow K\omega$ with $\omega \rightarrow \pi^+ \pi^- \pi^0$ [51]. Fig. 3b of Ref. [51] shows about 20 combinatorial-background events under the $B^- \rightarrow K^- \pi^+ \pi^- \pi^0$ signal peak for $\pi^+ \pi^- \pi^0$ mass in a 100-MeV-wide region and an integrated luminosity of about 0.75 ab^{-1} . This corresponds to about 53,000 events for the Belle II integrated luminosity of 50 ab^{-1} and our 3π mass range, which is roughly $450 < m_{3\pi} < 950$ MeV. This is the expected background yield in a prompt search. However, exploiting the DV signature suppresses the background by more than a factor of 10^5 [52–55]. Therefore, we conclude that the combinatorial background in this search is well below 1 event throughout the entire $m_{3\pi}$ range.

In addition, a potential source of peaking background is $B \rightarrow K\omega$ and $B \rightarrow K\eta$ decays, with the ω and η decaying to three pions. Based on Refs. [51] and [56], the numbers of events from these decays in a prompt analysis are similar to those of the combinatorial background. From this, we conclude that after the DV requirement, these backgrounds become negligible as well. Therefore, there is no need to reject events with $m_{3\pi}$ around the ω or η mass.

A more serious source of peaking background is $B^- \rightarrow K^- K_L$ with the long-lived K_L decaying to $\pi^+ \pi^- \pi^0$. The branching fraction of this decay chain is about 8.1×10^{-8} [45]. Given the K_L lifetime ($c\tau \approx 15 \text{ m}$), the reconstruction efficiency is about 0.12%. This results in about 5 events in the Belle II dataset. We use this estimated background to calculate a reduced sensitivity for m_a values in the 25-MeV-wide bin centered at 500 MeV. This bin is much wider than the $m_{3\pi}$ resolution, which is only a few MeV [57].

Peaking background may also arise from $B^- \rightarrow K^- K^{*0}(892)$ with $K^{*0}(892) \rightarrow K_S \pi^0$, and the long-lived K_S decaying to $\pi^+ \pi^-$ and forming a DV. The branching fraction for this decay chain is about 7×10^{-7} [45]. This background is efficiently removed by rejecting events with $m_{\pi^+ \pi^-} \approx M_{K_S}$ [52] and for which the $\pi^+ \pi^-$ momentum vector points from the interaction point to the DV. The impact of this K_S veto on the signal efficiency is small given the $m_{\pi^+ \pi^-}$ resolution of about 4 MeV [58], the momentum angular resolution of order a milliradian [59], and the DV position resolution of tens to hundreds of microns [59], depending on the DV position. If needed, further suppression may be obtained by rejecting events for which the invariant mass of the π^0 with the displaced $\pi^+ \pi^-$ pair, evaluated at the interaction point, is close to the peak of the $K^{*0}(892)$. Due to the $K^{*0}(892)$ width of about 50 MeV, this last cut would be more effective for low axion masses within our range of interest. We note also that at the limit of the experimental sensitivity, corresponding to highly long-lived axions, this background is exponentially suppressed by the relatively short ($c\tau \approx 2.7 \text{ cm}$) lifetime of the K_S . In our estimates we do not apply this requirement.

Thus, we conclude that the expected number of background events is below 1 event except for the 5 events in the region $m_{3\pi} \sim M_{K_L}$. The background yield in any narrow range corresponding to a signal peak with width of order a few MeV is even lower.

2. Efficiency

To estimate the signal efficiency, we use EvtGen [60] to generate $B^- \rightarrow K^- a(\pi^+ \pi^- \pi^0)$ events at the Belle II beam energies ($E_{e^-} = 7 \text{ GeV}$ and $E_{e^+} = 4 \text{ GeV}$). Simulated samples are produced for axion masses in range $450 \leq m_a \leq 1950$ MeV in steps of 25 MeV. For Fig. 3, samples are produced for 100 values of $c\tau \in [1\text{mm}, 1\text{m}]$. For calculation of the projected bounds, shown in Fig. 4, samples are produced for 73 values of $f_a \in [1, 10^5]$ GeV, with $c\tau$ determined from f_a according to Ref. [25]. Each sample contains 10^4 events. We calculate the effective efficiency for each sample as follows. Following Refs. [61, 62], we define the detector fiducial volume to be a cylinder of length $-40 < z < 120$ cm along the beam direction and maximal radius $r < 80$ cm in the transverse plane, excluding the radial region $r < 1$ cm in order to reject the promptly produced tracks. If a generated

¹ $a \rightarrow \gamma\pi\pi$ is allowed, but its branching ratio is very small for $m_a < 3m_\pi$. See the orange line of Fig. 2.

axion decays outside of the fiducial volume, its contribution to the efficiency is 0. For decays inside the fiducial volume, the radius-dependent track-detection efficiency ϵ_{det} is taken to be linearly decreasing from $r = 1$ cm ($\epsilon_{\text{det}} = 100\%$) to $r = 80$ cm ($\epsilon_{\text{det}} = 0$) [61, 62]. Finally, to take into account overall detection and reconstruction efficiencies, we multiply the efficiency by an overall factor of 22%, which we estimate from the Belle study of $B \rightarrow K\omega$ [51], to obtain the total efficiency, ϵ_{tot} . The total signal efficiency as a function of mean decay length and the axion mass is plotted in Fig. 3.

3. Projected bounds

We estimate the Belle II sensitivity to $B \rightarrow Ka(3\pi)$ in terms of the 95% confidence-level exclusion region in the plane of f_a vs m_a . We assume that 5×10^{10} pairs of $B\bar{B}$ are produced given the integrated luminosity of approximately 50 ab^{-1} . Given that the displaced search is essentially background-free, we take the exclusion region to be that for which the number of signal events satisfies $N_S \geq 3$. At $m_a \simeq m_{K_L}$, we require $N_S \geq 10$, because 5 background events are expected. The excluded region is shown shaded blue in Fig. 4, for the UV scales $\Lambda_{\text{UV}} = 1$ TeV and $\Lambda_{\text{UV}} = 10$ TeV.

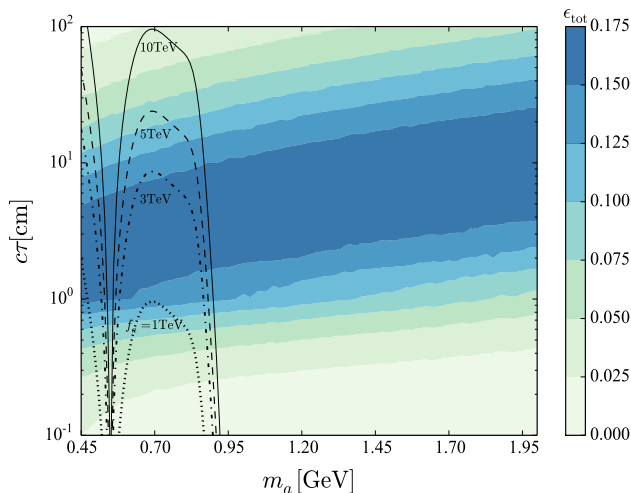


FIG. 3. Contours of the total efficiency for $B^- \rightarrow K^- a$ in the displaced $a \rightarrow \pi^+ \pi^- \pi^0$ channel as a function of the axion mass and $c\tau$ where τ is the proper lifetime of the axion.

B. Prompt $B^- \rightarrow K^- a(\gamma\gamma)$ signature

In the mass range $m_a < 3m_\pi \simeq 400$ MeV, the axion decays predominantly to $\gamma\gamma$. In Sec. III B 1, we use a recent BABAR search for an axion-like particle (ALP) in this channel [63] to derive bounds on the parameter space of the heavy QCD axion. In Sec. III B 2, we estimate the projected bounds at Belle II, allowing for longer axion lifetimes than those reported in Ref. [63].

1. Recasting of BABAR results

Fig. 4 of Ref. [63] shows the bound on the branching-fraction product $\text{BR}(B \rightarrow Ka) \times \text{BR}(a \rightarrow \gamma\gamma)$ that BABAR obtained with an integrated luminosity of 424 fb^{-1} as a function of m_a . The bounds are shown for four values of axion lifetime, $c\tau_{\text{BBR}} = 0, 0.1, 1, 10$ cm, and become weaker with increasing lifetime. To be conservative when recasting these bounds, we take the axion with m_a, f_a , and corresponding $c\tau(f_a, m_a)$ values to be excluded if BABAR excludes the same values of m_a and $\text{BR}(B \rightarrow Ka) \times \text{BR}(a \rightarrow \gamma\gamma)$ with an ALP lifetime that satisfies $c\tau_{\text{BBR}} \geq c\tau(f_a, m_a)$. The resulting bounds, shown in dark green in Fig.4, are naturally restricted by $c\tau < 10$ cm.

2. Projected results for Belle II

The $c\tau < 10$ cm restriction, necessitated when recasting the results of Ref. [63], is conservative given the size of the Belle II calorimeter and the limited boost of the axion. Therefore, we also derive the expected Belle II bounds from the $\gamma\gamma$ channel without this restriction, with the following procedure.

The impact of the background depends on the resolution of the signal peak in terms of the measured diphoton mass $m_{\gamma\gamma}$. For prompt axion decays, the detector resolution ranges from $\sigma_{m_{\gamma\gamma}} \approx 11$ MeV for $m_{\gamma\gamma} \approx 540$ MeV [64] to $\sigma_{m_{\gamma\gamma}} \approx 50$ MeV for $m_{\gamma\gamma} \approx 1860$ MeV [65]. However, displaced photons have an additional source of smearing: the angular resolution of the calorimeter is not sufficient for determining the point of origin of a photon. Therefore, the diphoton mass $m_{\gamma\gamma}$ must be calculated assuming that the photons are promptly produced at the interaction point. This results in a downward smearing of the measured diphoton mass, $m_{\gamma\gamma} \simeq m_a(1 - r/S)$, where $r = ct_a p_a/m_a$ is the flight distance of an axion with decay time t_a and momentum p_a , and S is the distance from the interaction point to the face of the calorimeter at the relevant point. As a result, the exponential distribution of the flight distance translates into the $m_{\gamma\gamma}$ distribution

$$\frac{dN}{dm_{\gamma\gamma}} = \frac{S}{p_a c\tau_a} \exp\left[\frac{S}{p_a c\tau_a}(m_{\gamma\gamma} - m_a)\right] \Theta(m_a - m_{\gamma\gamma}). \quad (5)$$

where Θ is the Heaviside step function. We take the typical values $p_a = 2.5$ GeV and $S = 120$ cm, and convolve this distribution with a Gaussian of width $\sigma_{m_{\gamma\gamma}} \simeq 0.02m_{\gamma\gamma}$, corresponding to the detector resolution [64, 65]. Our model reproduces very well the actual signal shape of the BABAR analysis for $m_a = 1$ GeV and $c\tau_a = 10$ cm, shown in p.18 of Ref. [66].

For given values of m_a and f_a we define the signal region to be the $m_{\gamma\gamma}$ region that contains 68% of the signal around the peak. Following Ref. [63], we take the efficiency for this decay chain to be 33% and calculate the expected signal yield N_S in the signal region. The expected background yield in this region, N_B , is calculated given the width of the signal region and two values of the assumed background density: 150 events per

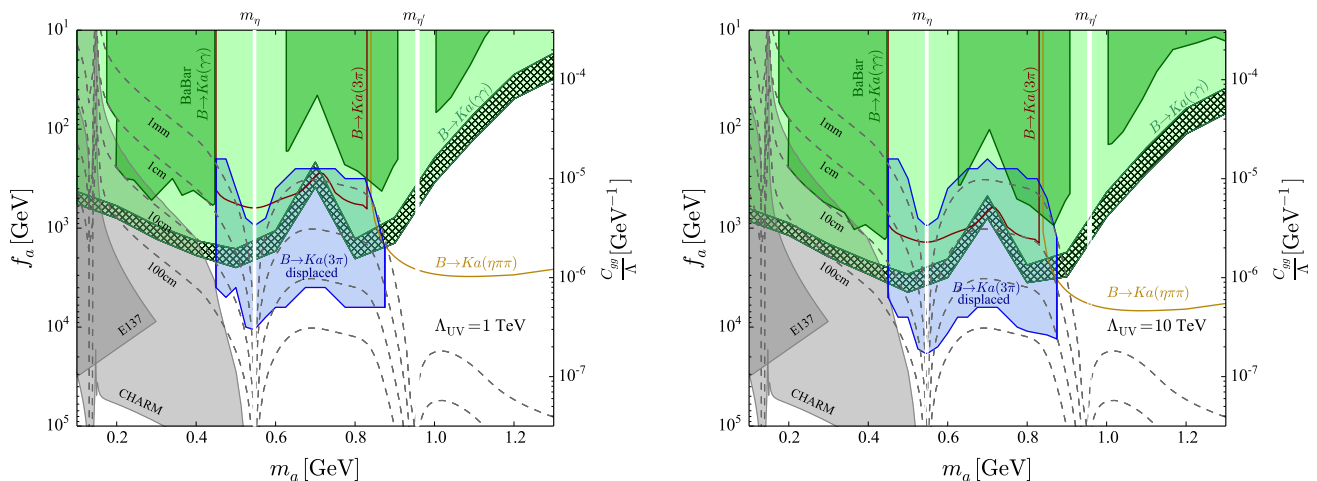


FIG. 4. In colors, we show the projected sensitivities and the new bound for $\Lambda_{UV} = 1$ TeV (left figure) and 10 TeV (right figure) respectively, using prompt and displaced analysis. The projections developed in this paper are the $B \rightarrow Ka(3\pi)$ displaced analysis (blue region) and $B \rightarrow Ka(\gamma\gamma)$ prompt analysis (green region). The green hatched region corresponds to a 10-fold variation of the estimated background rate in the $B \rightarrow Ka(\gamma\gamma)$ analysis. The bound of this channel is obtained by recasting the BABAR result [63] (dark green). The projections of $B \rightarrow Ka(3\pi)$ prompt analysis (magenta-outlined region) and $B \rightarrow Ka(3\pi)$ prompt analysis (yellow-outlined region) are from Ref. [44]. The grey regions refer to the present limits from B -decays, light meson decays and beam dump experiments. The dashed contours show the axion's $c\tau$ values.

MeV and 1500 events per MeV. These correspond to the background-level range shown in Fig. 1 of Ref. [63] for $m_a < 1.3$ GeV. Since the sensitivity on f_a scales as $N_B^{1/4}$, the 1-fold difference in background level has a relatively small impact on the projected limits. To avoid the background from $B \rightarrow K\pi^0(\gamma\gamma)$, N_S and N_B are calculated while excluding the mass range $125 < m_{\gamma\gamma} < 145$ MeV, corresponding roughly to $\pm 2\sigma$ around the π^0 mass. Finally, we take the sensitivity of the experiment to be f_a and m_a values for which $N_S/\sqrt{N_B} > 2$. The resulting projected limits are shown in light green in Fig. 4.

IV. DISCUSSION AND SUMMARY

In this paper we extract limits on the decay constant f_a of the heavy QCD axion as a function of its mass m_a . We recast $B \rightarrow Ka(\gamma\gamma)$ results from BABAR [63], and estimate the sensitivity of Belle II for this decay using the BABAR efficiency and background and accounting for mass smearing due to displaced axion decays, as well as for a displaced, $B \rightarrow Ka(3\pi)$ search.

The projected sensitivities, shown in Fig. 4 are calculated for two UV scales, $\Lambda_{UV} = 1$ TeV and $\Lambda_{UV} = 10$ TeV. The sensitivity is higher for higher choices of the UV scale because of large logarithmic corrections originating

from the renormalization group evolution. We find that the dependence on the exact nature of the UV model, parametrized by the coefficients A and B in Ref. [44], does not impact the results strongly. The variation of A and B have sizeable effects only for $\Lambda_{UV} = 1$ TeV, leading to at most $O(1)$ variation in the limits on f_a . To avoid clutter in Fig. 4, we chose optimistic values, $A = +3$ and $B = -3$.

We find that for axion mass in the range $450 \lesssim m_a \lesssim 900$ MeV, the decay $a \rightarrow 3\pi$ with a displaced-vertex signature is the best search channel, with sensitivities to the axion decay constant in the range $10^2 \lesssim f_a \lesssim 10^4$ GeV. Moreover, the $a \rightarrow \gamma\gamma$ channel can be used to probe the mass range $150 \lesssim m_a \lesssim 500$ MeV, covering the unconstrained range $10 \lesssim f_a \lesssim 10^3$ GeV of decay constant values.

ACKNOWLEDGMENTS

We thank Brian Shuve for corresponding about Ref. [63]. SC, VL, TO, and KT are supported by the US Department of Energy grant DE-SC0010102. TO and KT are also supported in part by JSPS KAKENHI 21H01086. EB and AS are supported by grants from the Israel Science Foundation, the US-Israel Binational Science Fund, the Israel Ministry of Science, and the Tel Aviv University Center for AI and Data Science.

[1] S. Weinberg, “A New Light Boson?,” *Phys. Rev. Lett.* **40** (1978) 223–226.

[2] F. Wilczek, “Problem of Strong P and T Invariance in the Presence of Instantons,” *Phys. Rev. Lett.* **40** (1978)

- 279–282.
- [3] R. Peccei and H. R. Quinn, “CP Conservation in the Presence of Instantons,” *Phys. Rev. Lett.* **38** (1977) 1440–1443.
- [4] R. Peccei and H. R. Quinn, “Constraints Imposed by CP Conservation in the Presence of Instantons,” *Phys. Rev. D* **16** (1977) 1791–1797.
- [5] G. ’t Hooft, “Symmetry Breaking Through Bell-Jackiw Anomalies,” *Phys. Rev. Lett.* **37** (1976) 8–11.
- [6] J. E. Kim and G. Carosi, “Axions and the Strong CP Problem,” *Rev. Mod. Phys.* **82** (2010) 557–602, [arXiv:0807.3125 \[hep-ph\]](#). [Erratum: *Rev. Mod. Phys.* **91**, 049902 (2019)].
- [7] **Particle Data Group** Collaboration, P. Zyla *et al.*, “Review of Particle Physics,” *PTEP* **2020** no. 8, (2020) 083C01.
- [8] P. Agrawal and K. Howe, “Factoring the Strong CP Problem,” *JHEP* **12** (2018) 029, [arXiv:1710.04213 \[hep-ph\]](#).
- [9] M. Kamionkowski and J. March-Russell, “Planck scale physics and the Peccei-Quinn mechanism,” *Phys. Lett. B* **282** (1992) 137–141, [arXiv:hep-th/9202003](#).
- [10] R. Holman, S. D. H. Hsu, T. W. Kephart, E. W. Kolb, R. Watkins, and L. M. Widrow, “Solutions to the strong CP problem in a world with gravity,” *Phys. Lett. B* **282** (1992) 132–136, [arXiv:hep-ph/9203206](#).
- [11] S. M. Barr and D. Seckel, “Planck scale corrections to axion models,” *Phys. Rev. D* **46** (1992) 539–549.
- [12] S. Ghigna, M. Lusignoli, and M. Roncadelli, “Instability of the invisible axion,” *Phys. Lett. B* **283** (1992) 278–281.
- [13] J. Bjorken, S. Ecklund, W. Nelson, A. Abashian, C. Church, B. Lu, L. Mo, T. Nunamaker, and P. Rassmann, “Search for Neutral Metastable Penetrating Particles Produced in the SLAC Beam Dump,” *Phys. Rev. D* **38** (1988) 3375.
- [14] J. Blumlein *et al.*, “Limits on neutral light scalar and pseudoscalar particles in a proton beam dump experiment,” *Z. Phys. C* **51** (1991) 341–350.
- [15] **CHARM** Collaboration, F. Bergsma *et al.*, “Search for Axion Like Particle Production in 400-{GeV} Proton - Copper Interactions,” *Phys. Lett. B* **157** (1985) 458–462.
- [16] **CAST** Collaboration, V. Anastassopoulos *et al.*, “New CAST Limit on the Axion-Photon Interaction,” *Nature Phys.* **13** (2017) 584–590, [arXiv:1705.02290 \[hep-ex\]](#).
- [17] G. G. Raffelt, “Astrophysical axion bounds,” *Lect. Notes Phys.* **741** (2008) 51–71, [arXiv:hep-ph/0611350](#).
- [18] G. Raffelt, *Stars as laboratories for fundamental physics: The astrophysics of neutrinos, axions, and other weakly interacting particles*. 5, 1996.
- [19] A. Friedland, M. Giannotti, and M. Wise, “Constraining the Axion-Photon Coupling with Massive Stars,” *Phys. Rev. Lett.* **110** no. 6, (2013) 061101, [arXiv:1210.1271 \[hep-ph\]](#).
- [20] H. Fukuda, K. Harigaya, M. Ibe, and T. T. Yanagida, “Model of visible QCD axion,” *Phys. Rev. D* **92** no. 1, (2015) 015021, [arXiv:1504.06084 \[hep-ph\]](#).
- [21] P. Agrawal, G. Marques-Tavares, and W. Xue, “Opening up the QCD axion window,” *JHEP* **03** (2018) 049, [arXiv:1708.05008 \[hep-ph\]](#).
- [22] M. K. Gaillard, M. B. Gavela, R. Houtz, P. Quilez, and R. Del Rey, “Color unified dynamical axion,” *Eur. Phys. J. C* **78** no. 11, (2018) 972, [arXiv:1805.06465 \[hep-ph\]](#).
- [23] T. Gherghetta, V. V. Khoze, A. Pomarol, and Y. Shirman, “The Axion Mass from 5D Small Instantons,” *JHEP* **03** (2020) 063, [arXiv:2001.05610 \[hep-ph\]](#).
- [24] F. Takahashi and W. Yin, “Heavy QCD axion inflation,” [arXiv:2105.10493 \[hep-ph\]](#).
- [25] D. Aloni, Y. Soreq, and M. Williams, “Coupling QCD-Scale Axionlike Particles to Gluons,” *Phys. Rev. Lett.* **123** no. 3, (2019) 031803, [arXiv:1811.03474 \[hep-ph\]](#).
- [26] H. Georgi, D. B. Kaplan, and L. Randall, “Manifesting the Invisible Axion at Low-energies,” *Phys. Lett. B* **169** (1986) 73–78.
- [27] W. A. Bardeen, R. D. Peccei, and T. Yanagida, “CONSTRAINTS ON VARIANT AXION MODELS,” *Nucl. Phys. B* **279** (1987) 401–428.
- [28] D. S. M. Alves and N. Weiner, “A viable QCD axion in the MeV mass range,” *JHEP* **07** (2018) 092, [arXiv:1710.03764 \[hep-ph\]](#).
- [29] S. Gori, G. Perez, and K. Tobioka, “KOTO vs. NA62 Dark Scalar Searches,” *JHEP* **08** (2020) 110, [arXiv:2005.05170 \[hep-ph\]](#).
- [30] **E949** Collaboration, A. V. Artamonov *et al.*, “Search for the decay K^+ to π^+ gamma gamma in the π^+ momentum region $P > 213$ MeV/c,” *Phys. Lett. B* **623** (2005) 192–199, [arXiv:hep-ex/0505069](#).
- [31] **NA62** Collaboration, C. Lazzeroni *et al.*, “Study of the $K^\pm \rightarrow \pi^\pm \gamma \gamma$ decay by the NA62 experiment,” *Phys. Lett. B* **732** (2014) 65–74, [arXiv:1402.4334 \[hep-ex\]](#).
- [32] **KTeV** Collaboration, E. Abouzaid *et al.*, “Final Results from the KTeV Experiment on the Decay $K_L \rightarrow \pi^0 \gamma \gamma$,” *Phys. Rev. D* **77** (2008) 112004, [arXiv:0805.0031 \[hep-ex\]](#).
- [33] **KOTO** Collaboration, J. K. Ahn *et al.*, “Search for the $K_L \rightarrow \pi^0 \nu \bar{\nu}$ and $K_L \rightarrow \pi^0 X^0$ decays at the J-PARC KOTO experiment,” *Phys. Rev. Lett.* **122** no. 2, (2019) 021802, [arXiv:1810.09655 \[hep-ex\]](#).
- [34] M. Bauer, M. Neubert, S. Renner, M. Schnubel, and A. Thamm, “Consistent treatment of axions in the weak chiral Lagrangian,” [arXiv:2102.13112 \[hep-ph\]](#).
- [35] **PIENU** Collaboration, A. Aguilar-Arevalo *et al.*, “Search for heavy neutrinos in $\pi \rightarrow \mu \nu$ decay,” *Phys. Lett. B* **798** (2019) 134980, [arXiv:1904.03269 \[hep-ex\]](#).
- [36] D. Pocanic *et al.*, “Precise measurement of the $\pi^+ \rightarrow \pi^0 e^+ \nu$ branching ratio,” *Phys. Rev. Lett.* **93** (2004) 181803, [arXiv:hep-ex/0312030](#).
- [37] W. Altmannshofer, S. Gori, and D. J. Robinson, “Constraining axionlike particles from rare pion decays,” *Phys. Rev. D* **101** no. 7, (2020) 075002, [arXiv:1909.00005 \[hep-ph\]](#).
- [38] **GlueX** Collaboration, H. Al Gholi *et al.*, “Measurement of the beam asymmetry Σ for π^0 and η photoproduction on the proton at $E_\gamma = 9$ GeV,” *Phys. Rev. C* **95** no. 4, (2017) 042201, [arXiv:1701.08123 \[nucl-ex\]](#).
- [39] D. Aloni, C. Fanelli, Y. Soreq, and M. Williams, “Photoproduction of Axionlike Particles,” *Phys. Rev. Lett.* **123** no. 7, (2019) 071801, [arXiv:1903.03586 \[hep-ph\]](#).
- [40] **OPAL** Collaboration, G. Abbiendi *et al.*, “Multiphoton production in $e^+ e^-$ collisions at $s^{**}(1/2) = 181$ -GeV to 209-GeV,” *Eur. Phys. J. C* **26** (2003) 331–344,

- arXiv:hep-ex/0210016.
- [41] S. Knapen, T. Lin, H. K. Lou, and T. Melia, “Searching for Axionlike Particles with Ultraperipheral Heavy-Ion Collisions,” *Phys. Rev. Lett.* **118** no. 17, (2017) 171801, arXiv:1607.06083 [hep-ph].
- [42] CMS Collaboration, A. M. Sirunyan *et al.*, “Search for low mass vector resonances decaying into quark-antiquark pairs in proton-proton collisions at $\sqrt{s} = 13$ TeV,” *JHEP* **01** (2018) 097, arXiv:1710.00159 [hep-ex].
- [43] A. Mariotti, D. Redigolo, F. Sala, and K. Tobioka, “New LHC bound on low-mass diphoton resonances,” *Phys. Lett. B* **783** (2018) 13–18, arXiv:1710.01743 [hep-ph].
- [44] S. Chakraborty, M. Kraus, V. Loladze, T. Okui, and K. Tobioka, “Heavy QCD Axion in $b \rightarrow s$ transition: Enhanced Limits and Projections,” arXiv:2102.04474 [hep-ph].
- [45] Particle Data Group Collaboration, P. A. Zyla *et al.*, “Review of Particle Physics,” *PTEP* **2020** no. 8, (2020) 083C01.
- [46] P. Ball and R. Zwicky, “ $B_{d,s} \rightarrow \rho, \omega, K^*, \phi$ decay form-factors from light-cone sum rules revisited,” *Phys. Rev. D* **71** (2005) 014029, arXiv:hep-ph/0412079.
- [47] P. Ball and R. Zwicky, “New results on $B \rightarrow \pi, K, \eta$ decay formfactors from light-cone sum rules,” *Phys. Rev. D* **71** (2005) 014015, arXiv:hep-ph/0406232.
- [48] E. Izaguirre, T. Lin, and B. Shuve, “Searching for Axionlike Particles in Flavor-Changing Neutral Current Processes,” *Phys. Rev. Lett.* **118** no. 11, (2017) 111802, arXiv:1611.09355 [hep-ph].
- [49] B. Batell, M. Pospelov, and A. Ritz, “Multi-lepton Signatures of a Hidden Sector in Rare B Decays,” *Phys. Rev. D* **83** (2011) 054005, arXiv:0911.4938 [hep-ph].
- [50] BaBar Collaboration, J. P. Lees *et al.*, “Search for $B \rightarrow K^{(*)} \nu \bar{\nu}$ and invisible quarkonium decays,” *Phys. Rev. D* **87** no. 11, (2013) 112005, arXiv:1303.7465 [hep-ex].
- [51] Belle Collaboration, V. Chobanova *et al.*, “Measurement of branching fractions and CP violation parameters in $B \rightarrow \omega K$ decays with first evidence of CP violation in $B^0 \rightarrow \omega K_S^0$,” *Phys. Rev. D* **90** no. 1, (2014) 012002, arXiv:1311.6666 [hep-ex].
- [52] BaBar Collaboration, J. P. Lees *et al.*, “Search for Long-Lived Particles in e^+e^- Collisions,” *Phys. Rev. Lett.* **114** no. 17, (2015) 171801, arXiv:1502.02580 [hep-ex].
- [53] Belle Collaboration, D. Liventsev *et al.*, “Search for heavy neutrinos at Belle,” *Phys. Rev. D* **87** no. 7, (2013) 071102, arXiv:1301.1105 [hep-ex]. [Erratum: *Phys. Rev. D* **95**, 099903 (2017)].
- [54] L. Lee, C. Ohm, A. Soffer, and T.-T. Yu, “Collider Searches for Long-Lived Particles Beyond the Standard Model,” *Prog. Part. Nucl. Phys.* **106** (2019) 210–255, arXiv:1810.12602 [hep-ph].
- [55] J. Alimena *et al.*, “Searching for long-lived particles beyond the Standard Model at the Large Hadron Collider,” *J. Phys. G* **47** no. 9, (2020) 090501, arXiv:1903.04497 [hep-ex].
- [56] Belle Collaboration, C. T. Hoi *et al.*, “Evidence for Direct CP Violation in $B^\pm \rightarrow \eta h^\pm$ and Observation of $B^0 \rightarrow \eta K^0$,” *Phys. Rev. Lett.* **108** (2012) 031801, arXiv:1110.2000 [hep-ex].
- [57] Belle Collaboration, C. H. Wang *et al.*, “Measurement of charmless B Decays to eta K* and eta rho,” *Phys. Rev. D* **75** (2007) 092005, arXiv:hep-ex/0701057.
- [58] Belle Collaboration, D. Epifanov *et al.*, “Study of tau- \rightarrow K(S) pi- nu(tau) decay at Belle,” *Phys. Lett. B* **654** (2007) 65–73, arXiv:0706.2231 [hep-ex].
- [59] BaBar, Belle Collaboration, A. J. Bevan *et al.*, “The Physics of the B Factories,” *Eur. Phys. J. C* **74** (2014) 3026, arXiv:1406.6311 [hep-ex].
- [60] D. J. Lange, “The EvtGen particle decay simulation package,” *Nucl. Instrum. Meth. A* **462** (2001) 152–155.
- [61] C. O. Dib, J. C. Helo, M. Nayak, N. A. Neill, A. Soffer, and J. Zamora-Saa, “Searching for a sterile neutrino that mixes predominantly with ν_τ at B factories,” *Phys. Rev. D* **101** no. 9, (2020) 093003, arXiv:1908.09719 [hep-ph].
- [62] S. Dey, C. O. Dib, J. Carlos Helo, M. Nayak, N. A. Neill, A. Soffer, and Z. S. Wang, “Long-lived light neutralinos at Belle II,” *JHEP* **02** (2021) 211, arXiv:2012.00438 [hep-ph].
- [63] BaBar Collaboration, J. P. Lees *et al.*, “Search for an Axion-Like Particle in B Meson Decays,” arXiv:2111.01800 [hep-ex].
- [64] BaBar Collaboration, “Belle ii $m_{\gamma\gamma}$ plots,” <https://docs.belle2.org/record/1589/files/BELLE2-NOTE-PL-2019-019.pdf>.
- [65] BaBar Collaboration, J. P. Lees *et al.*, “Search for the Decay $D^0 \rightarrow \gamma\gamma$ and Measurement of the Branching Fraction for $D^0 \rightarrow \pi^0 \pi^0$,” *Phys. Rev. D* **85** (2012) 091107, arXiv:1110.6480 [hep-ex].
- [66] B. Shuve, “SEARCH FOR AN AXIONLIKE PARTICLE IN $B^\pm \rightarrow K^\pm a$, $a \rightarrow \gamma\gamma$ at BaBar experiment.” https://indico.cern.ch/event/868940/contributions/3814877/attachments/2080491/3496082/Shuve_ICHEP_BABAR_ALP.pdf. ICHEP 2020, 28 July 2020.